

(³He,α) Reaction on ⁸⁹Y and ⁸⁶Kr at 18 MeV*

C. M. FOU† AND R. W. ZURMÜHLE

Department of Physics, University of Pennsylvania, Philadelphia, Pennsylvania 19104

(Received 19 April 1968)

Neutron hole states in $N=49$ nuclei were studied with the (³He,α) reaction on ⁸⁹Y and ⁸⁶Kr. Spectroscopic information was obtained from a distorted-wave Born-approximation analysis. Various optical potential wells were used. The results were compared and found to be in good agreement with each other. In ⁸⁹Y, the ground state and the first excited state (0.40 MeV) are excited by $1g_{9/2}$ neutron pickup. The coupling of the unpaired $2p_{1/2}$ proton to the $1g_{9/2}$ neutron hole yields 4^- and 5^- states. Assuming that these two states represent the total $T < g_{9/2}$ neutron pickup strength in ⁸⁹Y, the sum of their spectroscopic factors is normalized to 10. Using the same normalization factor for ⁸⁶Kr states, the spectroscopic factor for the ground state excited by $1g_{9/2}$ neutron pickup represents only 60% of the total $T < g_{9/2}$ neutron pickup strength. Two other possible $\frac{3}{2}^+$ neutron hole states were observed at 1.89- and 2.03-MeV excitation. Spectroscopic information about other neutron hole states observed is also presented.

I. INTRODUCTION

THE purpose of this experiment is to study the neutron configurations of $N=50$ nuclei and the energy levels of the neutron hole states in $N=49$ nuclei. The interesting points of this investigation are whether or not $N=50$ is a good closed shell, how the major shell mixing depends on the number of protons in the nucleus, and how the energy levels of neutron hole states change with proton number in $N=49$ nuclei.

The (³He,α) reaction is particularly suited for this type of study because of its high reaction Q value. It allows one to see states up to rather high excitation energies without using elaborate particle-identification counter telescopes. So far, (³He,α) reaction studies have been performed on ⁹⁰Zr,¹ ⁹²Mo, and ⁸⁸Sr.² The present experiment on ⁸⁹Y and ⁸⁶Kr yields more information on $N=50$ nuclei.

Previously, levels in ⁸⁶Kr had been studied in ⁸⁴Kr(d,p)⁸⁵Kr and ⁸⁶Kr(d,t)⁸⁵ reactions.^{3,4} Five levels up to 2.2-MeV excitation were reported in the (d,t) work but no distorted-wave Born-approximation (DWBA) analysis was performed. However, in the (d,t) reaction an $l=1$ angular momentum transfer was deduced for the 1.12-MeV state from the close similarity between the angular distributions of the tritons leading to this state and to the 0.305-MeV state which is known to be the $\frac{1}{2}^-$ isomeric state.⁵ Levels in ⁸⁹Y have been studied in ⁸⁹Y(p,d)⁸⁸Y reaction.⁶ Spectroscopic information deduced from the DWBA analysis for eight excited states was reported. Comparison with the results obtained in

the present experiment will be made in the following sections.

II. EXPERIMENTAL TECHNIQUE

The experiment was performed with the 18-MeV ³He beam from the University of Pennsylvania Tandem Van de Graaff accelerator in a 24-in. scattering chamber, the design and operation of which have been described elsewhere.⁷ A solid-state detector array consisting of eight 500-μm-thick silicon surface-barrier detectors placed at 10° intervals was used to detect the α particles from the reactions. Angular distributions were measured between 15° and 90° in 5° steps. The acceptance angle of the detector was about 1°. The angular positions of the detectors were known to $\pm \frac{1}{10}^\circ$ accuracy. Details of the experimental procedures were the same as described earlier.⁸

The ⁸⁹Y target was prepared by vacuum evaporation of chemically pure natural yttrium metal onto a 20 μg/cm² carbon foil. The approximate thickness of this target was 100 μg/cm².

The ⁸⁶Kr target was contained in a gas cell with Mylar windows of 0.00015 in. thickness in which the 18-MeV ³He beam loses approximately 140 keV. The cell was filled to a pressure of 2 psi with 99% isotopically enriched ⁸⁶Kr gas.⁹ To reduce damage to the cell window from the heat generated by beam bombardment a reciprocating rotational motion was applied to the cell.¹⁰

III. EXPERIMENTAL RESULTS**A. ⁸⁶Kr(³He,α)⁸⁶Kr**

The following levels were observed in this reaction: the ground state (g.s.), the 0.31-, 1.05-, 1.14-, 1.89-, 2.03-, and 2.38-MeV states. There is a systematic dif-

* Supported by the National Science Foundation.

† Present address: Department of Physics, University of Delaware, Newark, Delaware 19711.

¹ C. M. Fou, R. W. Zurmühle, and J. M. Joyce, Phys. Rev. **155**, 1248 (1967).² G. Bassani (private communication).³ G. W. Wheeler, R. B. Schwartz, and W. W. Watson, Phys. Rev. **92**, 121 (1953).⁴ B. Rosner and E. J. Schneid, Nucl. Phys. **82**, 182 (1966).⁵ *Nuclear Data Sheets*, compiled by K. Way *et al.* (Printing and Publishing Office, National Academy of Sciences—National Research Council, Washington 25, D. C., 1964).⁶ C. A. Ludemann, C. D. Goodman, and W. H. Kelly, Bull. Am. Phys. Soc. **10**, 122 (1965).⁷ R. W. Zurmühle, Nucl. Instr. Methods **36**, 168 (1965).⁸ C. M. Fou and R. W. Zurmühle, Phys. Rev. **140**, B1283 (1965).⁹ ⁸⁶Kr gas supplied by Monsanto Research Corporation, Miamisburg, Ohio.¹⁰ R. W. Zurmühle and C. M. Fou, Nucl. Instr. Methods **54**, 151 (1967).

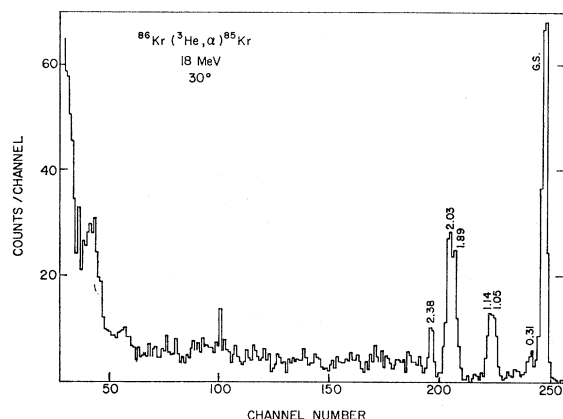


FIG. 1. α -particle spectrum from $^{86}\text{Kr}(^3\text{He}, \alpha)^{86}\text{Kr}$ reaction taken at 30° . The numbers above the peaks indicate the excitation energies in MeV.

ference between the excitation energies determined in the $^{86}\text{Kr}(d, t)^{86}\text{Kr}$ work⁴ and the present values (see Table I). The fractional difference in excitation energies between these values is roughly constant around 8%. A similar discrepancy exists between the value (710 ± 40 keV) obtained in the (d, t) work⁴ for the difference of Q values for $^{86}\text{Kr}(d, t)^{86}\text{Kr}$ and $^{84}\text{Kr}(d, t)^{84}\text{Kr}$ and the value obtained from the latest mass table (670 ± 18 keV).¹¹

The excitation energies in the present experiment were determined by using the known $^{86}\text{Kr}(^3\text{He}, \alpha)^{86}\text{Kr}$ g.s.-reaction Q value of 10.73 ± 0.015 MeV.¹¹ Linear interpolation between the peaks corresponding to the strongly excited g.s. of ^{86}Kr and the elastic scattering of ^3He by ^{86}Kr was made to determine the energy differences between the g.s. and various excited states. The excitation energies were then calculated kinematically from these energy differences. Energy losses in the gas and cell windows were taken into account in the energy interpolation and kinematic calculation. In the 30° and 80° spectra, the peak positions could be determined within half of a channel which corresponded to about 25 keV. The differences between the excitation

TABLE I. Comparison of excitation energies of levels in ^{86}Kr observed in $^{86}\text{Kr}(d, t)^{86}\text{Kr}$ reaction (Ref. 4) and the present $^{86}\text{Kr}(^3\text{He}, \alpha)^{86}\text{Kr}$ reaction.

Excitation energy (MeV)	
(d, t)	$(^3\text{He}, \alpha)$
g.s.	g.s.
0.305	0.31
1.12	1.05
	1.14
1.44	
2.05	1.89
2.20	2.03
	2.38

¹¹ J. H. E. Mattauch, W. Thiele, and A. H. Wapstra, Nucl. Phys. **67**, 1 (1965).

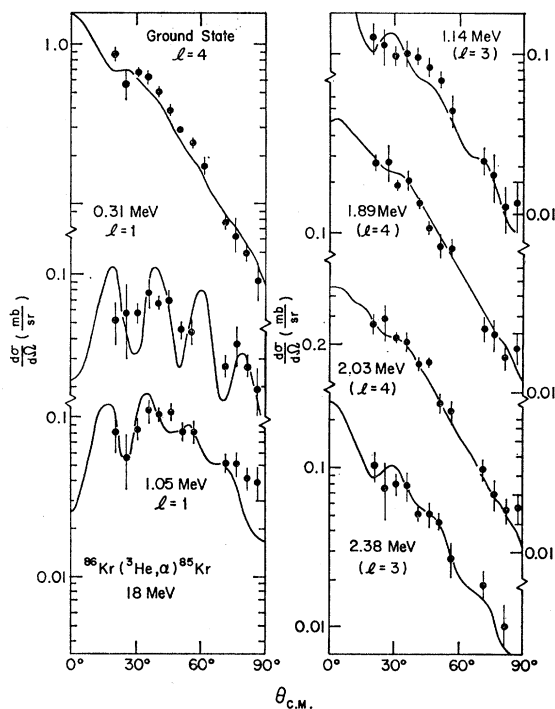


FIG. 2. Angular distribution of α particles from $^{86}\text{Kr}(^3\text{He}, \alpha)^{86}\text{Kr}$ reaction leading to various low-lying states in ^{86}Kr . The modified deep optical potential wells were used.

energies calculated from these two spectra were less than 30 keV. The averaged values are presented here.

The ^{86}Kr g.s., $\frac{3}{2}^+$,⁵ is very strongly excited by pickup of a $g_{9/2}$ neutron. The 1.05- and 1.14-MeV states as well as the 1.89- and 2.03-MeV states were not completely resolved. However, differential cross sections could be extracted by fitting the shape of the strongly excited g.s. peak to the pairs of unresolved peaks. The uncertainties of the excitation energies given here are about 50 keV. These uncertainties are mostly due to detector and electronic resolution. Since four detectors are sharing the same analog-to-digital converter, the noise of all four detectors contributes and affects all four 256-channel spectra. The over-all energy resolution was approximately 150 keV. A spectrum taken at 30° is shown in Fig. 1. The 1.44-MeV state reported in the (d, t) work⁴ cannot be identified. Angular distributions of α particles leading to various states in ^{86}Kr are shown in Fig. 2 together with DWBA predictions.

B. $^{89}\text{Y}(^3\text{He}, \alpha)^{88}\text{Y}$

The spin and parity of the ^{89}Y g.s. are $\frac{1}{2}^-$.⁵ According to the shell model the unpaired nucleon is a $2p_{1/2}$ proton. When a $1g_{9/2}$ neutron is picked up the proton and the neutron hole can form 4^- and 5^- states in ^{88}Y . The g.s. and the 0.25-MeV state are strongly excited in this reaction and are likely candidates for these two configurations. Other levels were identified at excitation energies of 0.40, 0.75, 1.25, 1.60, and 1.73 MeV. These

TABLE II. Optical-potential parameters used in the DWBA analysis. In the "Remarks" column, the sources of these parameter sets are given. All the parameters are defined the same as in Ref. 17. The energies in parentheses are the incident energies of the projectile on the target nuclei indicated. All parameters were obtained from the analysis of elastic scattering data. Parameter sets ^3He -142 and α -183 the modified parameter sets used by Stock *et al.* to fulfill the criterion for better DWBA ($^3\text{He}, \alpha$) predictions.

	V (MeV)	r_p (F)	a_p (F)	W (MeV)	r_w (F)	a_w (F)	V_{s0} (MeV)	r_o (F)	Remarks	Ref.
^3He -31	31.3	1.67	0.58	16.1	1.67	0.58	0	1.4	^{58}Ni (18 MeV)	8
^3He -142	142.4	1.362	0.65	12.67	1.755	0.781	8.05	1.4	^{52}Cr (19.5 MeV)	16
^3He -173	173.0	1.14	0.723	17.6	1.60	0.81	0	1.4	Consistent set	18
^3He -175	175.0	1.13	0.735	18.89	1.56	0.860	0	1.4	^{92}Zr (51 MeV)	19
^3He -196	196.9	1.04	0.811	17.37	1.60	0.797	0	1.4	^{92}Zr (51 MeV)	19
α -94	94.5	1.475	0.561	14.7	1.475	0.561	0	1.4	^{90}Zr (34.4 MeV)	18
α -183	183.7	1.4	0.56	26.0	1.48	0.56	0	1.4	^{50}Ti (30.5 MeV)	16
α -187	187.3	1.444	0.523	22.3	1.444	0.523	0	1.3	Zr (24.7 MeV)	15
α -228	228.0	1.366	0.577	23.3	1.242	0.577	0	1.4	^{90}Zr (34.4 MeV)	18

levels have also been seen in the (p, d) reaction.⁶ [In the recent $^{89}\text{Y}(p, d\gamma)^{88}\text{Y}$ reaction study by Goodman,¹² it was found that at 1.25-MeV excitation there is an unresolved doublet (1.217 and 1.278 MeV). A weakly excited state at 0.695-MeV excitation is also observed. In the present experiment neither the 0.695- nor the 1.217-MeV state could be identified.] The excitation energies determined in these two experiments agree to within experimental uncertainties of ± 50 keV. An α -particle spectrum is shown in Fig. 3. The over-all energy resolution was about 100 keV.

Experimental angular distributions are shown in Fig. 4 together with the DWBA predictions.

IV. DWBA ANALYSIS

The DWBA analysis was carried out using the Oak Ridge National Laboratory computer code JULIE.¹³ The zero-range approximation and local potentials were used throughout. ^3He elastic scattering angular distributions in both ^{89}Y and ^{86}Kr were measured, but the angular distributions show little structure and it was not possible to derive unambiguous optical-model parameters from these angular distributions. However, if the optical model is to be applied to the description of particle-

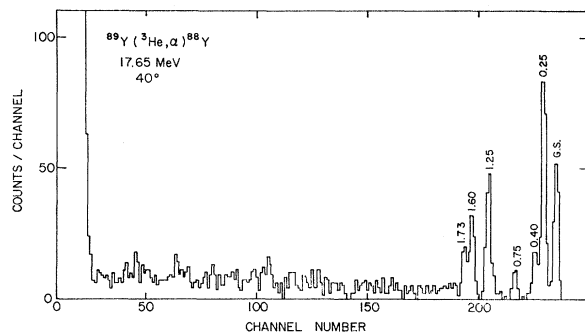


FIG. 3. α -particle spectrum from $^{89}\text{Y}(^3\text{He}, \alpha)^{88}\text{Y}$ reaction taken at 40° . The numbers above the peaks indicate the excitation energies in MeV.

¹² C. D. Goodman (private communication).

¹³ R. M. Drisko (private communication).

nucleus scattering, one generally assumes that the parameters which characterize the optical potential should be a constant, or a slowly varying function of the mass of the nucleus and the incident energy of the particle. This assumption has been justified by optical-model analyses of many elastic scattering experiments with a wide range of incident particle energies and target masses.¹⁴ Therefore, we used parameters that were determined from the analysis of elastic scattering of He^3 by zirconium at higher bombarding energies and by nickel and chromium at 18 MeV. Optical-potential parameters for the outgoing α -particle channel were

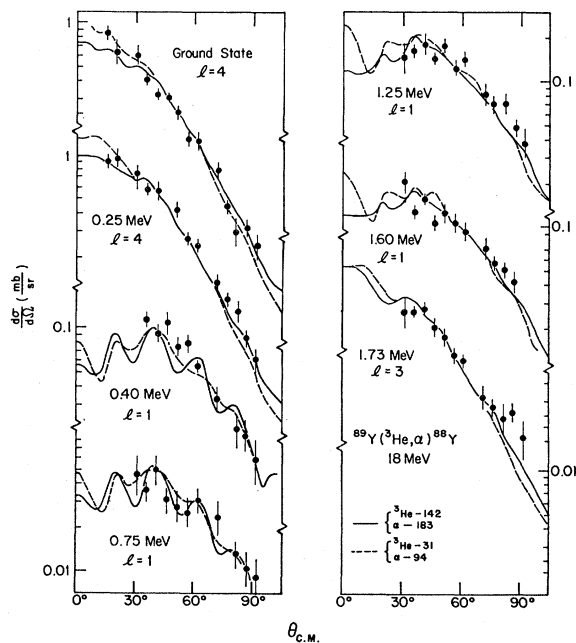


FIG. 4. Experimental angular distribution of α particles from $^{89}\text{Y}(^3\text{He}, \alpha)^{88}\text{Y}$ leading to various low-lying states in ^{88}Y are compared with the DWBA predictions assuming the angular momentum transfer indicated. The solid curves were obtained using the modified deep ^3He well. The broken curves were obtained using the shallow ^3He well.

¹⁴ P. E. Hodgson, *The Optical Model of Elastic Scattering* (Oxford University Press, London, 1963).

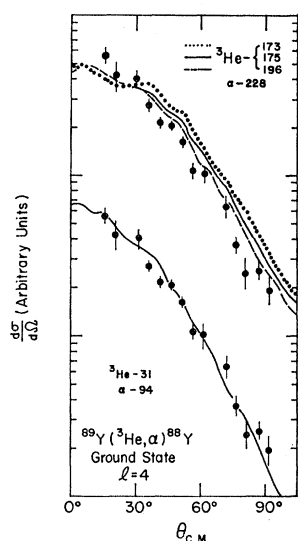


FIG. 5. DWBA predictions assuming an $l=4$ (${}^3\text{He}, \alpha$) transition to the g.s. of ${}^{88}\text{Y}$ are compared with the experimental data. The three curves in the upper portion of the figure are obtained using the searched deep ${}^3\text{He}$ optical-potential parameters. In all three cases the combination with α -228 yielded better fits than with other α potentials. The curve in the lower portion of the figure was obtained using the searched shallow ${}^3\text{He}$ optical-potential parameters. All ${}^3\text{He}$ parameters and α parameters are tabulated in Table II.

taken from McFadden and Satchler.¹⁵ All the parameters are listed in Table II.¹⁶⁻¹⁹

If one assumes that the real optical potential of a composite projectile consisting of N nucleons is approximately N times that of a proton or neutron, the potential well is about 150–180 MeV deep for He^3 and 200–240 MeV deep for He^4 . However, it has been found previously¹ in a DWBA analysis that predictions using such sets of ${}^3\text{He}$ and α potentials are usually in poorer agreement with experimental data than predictions obtained using shallow wells (${}^3\text{He}$: $V_{\text{real}} \approx 30$ MeV, α : $V_{\text{real}} \approx 85$ MeV). To investigate this point further, DWBA calculations were performed using both the deep and shallow ${}^3\text{He}$ and α potentials for the angular distribution of α particles leading to the g.s. of ${}^{88}\text{Y}$. Since the spin and parity of this state is known to be 4^- , there is no ambiguity in assuming $l=4$ for the DWBA calculation. The results were compared with experimental data and are shown in Fig. 5. The predictions using the deep wells do not fall off as rapidly as the experimental angular distributions.

In a recent investigation of the applicability of the DWBA analysis to (${}^3\text{He}, \alpha$) reactions, Stock *et al.*,¹⁶ based on qualitative argument, made the suggestion

¹⁵ L. McFadden and G. R. Satchler, Nucl. Phys. **84**, 177 (1966).

¹⁶ R. Stock, R. Bock, P. David, H. H. Duhm, and T. Tamura, Nucl. Phys. **A104**, 136 (1967).

¹⁷ E. M. Kellogg and R. W. Zurmühle, Phys. Rev. **152**, 890 (1966).

¹⁸ R. H. Bassel (private communication).

¹⁹ C. R. Bingham and M. L. Halbert, Phys. Rev. **158**, 1085 (1967).

that in order to obtain good DWBA fits to the (${}^3\text{He}, \alpha$) reaction data, the potential for α particles must be chosen to be approximately equal to the sum of the optical potentials for ${}^3\text{He}$ and for neutrons. To prove this point, Stock *et al.* showed that the optical potentials for ${}^3\text{He}$ and α , which one usually obtains from parameter searches using elastic scattering data, do not fulfill the abovementioned relation. And, it turns out, the DWBA prediction using these potentials are in poor agreement with experimental data. An objective measurement of how well the predicted angular distribution agrees with the experimental one is the χ^2 , defined as

$$\chi^2 = \sum_{\Theta_j} \frac{|\sigma_{\text{theor}}(\Theta_j) - \sigma_{\text{expt}}(\Theta_j)|^2}{|\Delta\sigma_{\text{expt}}(\Theta_j)|^2}.$$

In an actual optical-potential-parameter search one tries to minimize the χ^2 value by varying the parameters. But now, to get good DWBA fits for (${}^3\text{He}, \alpha$) reaction data, one has to change the parameters in one (or both) of the optical potentials. In order to make these parameters not completely arbitrary, one has to require that after the change has been made the predicted elastic scattering angular distribution still agrees reasonably well with the experimental data. Consequently, two χ^2 values have to be minimized; one measures the agreement between the predicted and measured elastic scattering angular distribution, the other measures the agreement between the DWBA prediction and the (${}^3\text{He}, \alpha$) reaction data. Since the elastic scattering angular distribution of ${}^3\text{He}$ has less structure than that of α particles, it is easier to achieve a lower value for both χ^2 by varying the parameters of the optical potential of ${}^3\text{He}$. In doing so, Stock *et al.* obtained a set of parameters for ${}^3\text{He}$ hereafter called the modified ${}^3\text{He}$ optical potential. The parameters are listed in Table II. The real radius parameter is 1.36 F instead of 1.14 F and the real well depth is 142.4 MeV instead of 173 MeV. A spin-orbit potential with $V_{s.o.} = 8.05$ MeV is also included. Together with the optical potential for α particles (α -183 in Table II) this modified ${}^3\text{He}$ optical potential satisfies the criterion of Stock *et al.* almost perfectly.¹⁶

This modified ${}^3\text{He}$ optical potential was used with two sets of α -particle optical potentials in the DWBA calculation to predict the angular distribution of α particles from ${}^{89}\text{Y}({}^3\text{He}, \alpha){}^{88}\text{Y}$ g.s. reaction. One of the optical-potential-parameter sets for the exit channel was obtained by Stock *et al.* from the analysis of data on the elastic scattering α particles by ${}^{90}\text{Ti}$ at 30 MeV.¹⁶ The other parameter set was obtained by McFadden and Satchler from the analysis of data on the elastic scattering of α particles by ${}^{90}\text{Zr}$ at 24.7 MeV.¹⁵ Both DWBA predictions for $l=4$ transition fit the experimental data (Fig. 6) much better than predictions obtained with the unmodified ${}^3\text{He}$ optical potential (Fig. 5). It appears that the present DWBA analysis supports the criterion

obtained by Stock *et al.* for the best combination of ^3He and α potentials to be used successfully in the DWBA analysis of $(^3\text{He}, \alpha)$ reactions. In the case of shallow wells, searched parameters which best fit the elastic scattering angular distributions also satisfy the criterion and therefore can be used. In the case of deep wells, a modified ^3He optical potential with $r_v \approx 1.4 \text{ F}$ and $V_{s.o.} \approx 8 \text{ MeV}$ should be used.

V. SPECTROSCOPIC FACTORS

A. General

The spectroscopic factors were extracted using the separation-energy prescription. Wave functions of the transferred neutron were calculated from a real Woods-Saxon well. The radius and diffuseness parameters were 1.2 and 0.65 F, respectively. The well depth for the transferred neutron, which is assumed to be in a particular shell-model orbital, was adjusted to make the binding energy equal to the separation energy. The spectroscopic factor S was calculated using the following equation¹⁸:

$$\sigma_{\text{expt}} = NS\sigma_{\text{DWBA(JULIE)}}.$$

The factor N depends, in part, on the overlap of the ^3He and α -particle wave functions and the strength of interaction which binds the neutron to ^3He to form α particles. It also contains the spin statistical factor of ^3He and the neutron forming α particle. The theoretical value of N , if one assumes zero-range interaction, is 1.63. However, when S can be determined otherwise, N has been found empirically to be about 20–30 times greater than 1.63.^{20,21} This factor of 20–30 will be called the normalization factor in the following sections.

TABLE III. Summary of the DWBA analysis for states in ^{89}Y . Spectroscopic factors in column 3 were extracted using shallow optical potential wells. Those in columns 4 and 5 were extracted using deep optical potential wells with and without a spin-orbit term in the calculation of the bound-state wave function, respectively. The sum of the spectroscopic factors of the ground and 0.25-MeV states is normalized to 10.0 in columns 3 and 4, while in column 5 the sum of the spectroscopic factor of the 0.40- and 0.75-MeV states is normalized to 2.0.

Excitation energy (MeV)	$l(J^\pi)$	Spectroscopic factors		
		Shallow	Deep I	Deep II
0.00	4(4 ⁻)	4.2 ^a	4.4 ^a	3.5
0.25	4(5 ⁻)	5.8 ^a	5.6 ^a	4.4
0.40	1(1 ⁺)	1.5	1.3	1.4 ^a
0.75	1(0 ⁺)	0.6	0.6	0.6 ^a
1.25	1(2 ⁺)	2.2	2.1	2.0
1.60	1(1 ⁺)	1.7	1.6	1.5
1.73	3	1.3	1.3	

^a Normalized value.

²⁰ L. M. Blau, W. Parker Alford, D. Cline, and H. E. Gove, Nucl. Phys. **76**, 45 (1966).

²¹ D. E. Rundquist, M. K. Brussel, and A. I. Yavin, Phys. Rev. **168**, 1296 (1968).

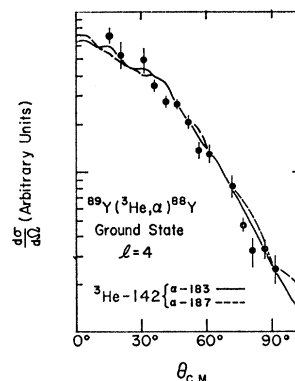


FIG. 6. DWBA predictions assuming an $l=4$ $(^3\text{He}, \alpha)$ transition to the g.s. of ^{89}Y . For the incident ^3He wave a modified optical potential which satisfies the criterion set by Stock *et al.* was used. Two different sets of α -particle optical-potential parameters were used. The results are very similar. The parameters are tabulated in Table II.

B. $^{89}\text{Y}(^3\text{He}, \alpha)^{89}\text{Y}$

Spectroscopic factors were extracted from DWBA predictions using both deep and shallow optical-potential wells. The values are listed in Table III. They are in agreement with each other within the extraction uncertainties, which are between ± 10 and $\pm 20\%$. These uncertainties depend on the over-all agreement between DWBA predictions and experimental data. The spectroscopic factors are normalized by assuming that the g.s. and the 0.25-MeV state in ^{89}Y are the only two states excited by pickup of a $g_{9/2}$ neutron from ^{89}Y . $T_{>}$ states excited by $g_{9/2}$ neutron pickup are expected to have very small spectroscopic factors. According to French and Macfarlane,²² the sum of the spectroscopic factors for $T_{>}$ states is the proton occupation number divided by $N-Z+1$. Since $N-Z+1 \geq 12$ for ^{89}Y and ^{86}Kr ($N-Z+1=12$ for ^{89}Y and 13 for ^{86}Kr) and the $g_{9/2}$ proton occupation number is expected to be less than 2, the sum of the spectroscopic factors for $T_{> \frac{9}{2}^+}$ neutron hole states is approximately 0.1–0.2 as compared to 10 for the total sum for $T_{>}$ and $T_{<}$ states. The error in normalizing the sum of the spectroscopic factors for $T_{< \frac{9}{2}^+}$ states to 10 is therefore only 1 or 2%. Consequently, the sum was normalized to 10.0, the maximum number of $g_{9/2}$ neutrons. The normalization factor obtained is 25 for the modified deep well and 19 for the shallow well. These values are consistent with the normalization factors obtained in many other DWBA analyses for $(^3\text{He}, \alpha)$ reactions.^{16,20,21} With this normalization, the sum of the spectroscopic factors of the 0.40- and 0.75-MeV states (both $l=1$) extracted using the modified deep well turns out to be 1.9 and that of the 1.25- and 1.60-MeV states to be 3.8. These numbers are consistent with the hypothesis that the neutrons in ^{89}Y fill the $N=50$ shell and the single proton occupies the $2p_{1/2}$ shell. The g.s. and the 0.25-MeV

²² J. B. French and M. H. Macfarlane, Nucl. Phys. **26**, 168 (1961).

PRESENT RESULTS		(p,d) (p,dγ) RESULTS	PRESENT RESULTS		⁹⁰ Zr (³ He,α) ⁸⁸ Zr REFERENCE	
ℓ	J ^π	J ^π	ℓ	J ^π	ℓ	J ^π
2.38	(3) (5/2 ⁻)				2.06	3 (5/2 ⁻)
2.03	(4) (3/2 ⁺)				1.84	1 (3/2 ⁺)
1.89	(4) (3/2 ⁺)	1.73 1.60	3 (3/2 ⁺) 1 (1 ⁺)		1.72	(3) (3/2 ⁺)
		1.25	1 (2 ⁺)		1.44	3 (5/2 ⁻)
1.05	(3) (5/2 ⁻)	1.217	1 (2 ⁺)		1.07	1 (3/2 ⁻)
	(1) (3/2 ⁻)	0.75	1 (0 ⁺)		0.59	1 (1/2 ⁻)
		0.695	1 (2 ⁺)			
0.31	1 (1/2 ⁻)	0.40	1 (1 ⁺)			
		0.25	5 ⁻			
	4 (3/2 ⁻)		4 (5 ⁻)			
			4 (4 ⁻)			
⁸⁵ Kr		⁸⁸ Y		⁸⁹ Zr		

FIG. 7. Low-lying neutron hole states in ⁸⁹Zr, ⁸⁸Y, and ⁸⁵Kr are compared. In ⁸⁸Y, states probably resulting from the coupling of the 2p_{1/2} proton with the same neutron hole are connected with a curly bracket. The approximate positions of neutron hole states are indicated. In ⁸⁵Kr, two candidates for g_{9/2} neutron hole states beside the g.s. are shown. Their excitation energies are 1.89 and 2.03 MeV.

state of ⁸⁸Y are then excited by 1g_{9/2} neutron pickup and the g_{9/2} neutron hole couples with the 2p_{1/2} proton to yield the 4⁻ and 5⁻ states. Similarly, the 0.40- and 0.75-MeV states are due to 2p_{1/2} neutron pickup and the 1.25- and 1.60-MeV states are due to 2p_{3/2} neutron pickup. As in ⁸⁹Zr, the 1f_{5/2} neutron hole state is probably split into several states.¹ The coupling with a 2p_{1/2} proton complicates the level scheme further and the 1f_{5/2} neutron hole states have not all been identified. The 1.73-MeV state, l=3, represents only 1.3 of the total strength of 6.0. Tentative spin assignments based upon the above assumption and the 2J+1 rule were made and are listed in Table III. These assignments are in agreement with the recent ⁸⁹Y(p,dγ) results¹² (Fig. 7).

Spectroscopic factors were also extracted from the deep-well DWBA predictions which included a spin-orbit term 25 times the Thomas term for the calculation

TABLE IV. Summary of the DWBA analysis for states in ⁸⁵Kr. The spectroscopic factor for the 0.31-MeV state is normalized to 2, implying that the total 2p_{1/2} neutron pickup strength is observed in this state. In column 4 a spin-orbit term was included in the calculation of the bound-state wave function.

Excitation energy (MeV)	l(J ^π)	Spectroscopic factors	
		Deep I	Deep II
0.00	4 (3/2 ⁺)	6.4	5.5
0.31	1 (1/2 ⁻)	2.0*	2.0*
1.05	1 (3/2 ⁻)	2.4	2.4
1.14	(3) (5/2 ⁻)	(1.5)	(1.8)
1.89	{ (3) (3/2 ⁻) (4) (3/2 ⁺)	{ (2.2) (1.8)	{ (2.7) (1.3)
2.03	{ (3) (5/2 ⁻) (4) (3/2 ⁺)	{ (2.5) (1.9)	{ (3.0) (1.4)
2.38	(3) (5/2 ⁻)	(0.7)	(0.9)

* Normalized value.

of the bound-state wave function. The extracted values are listed in Table III. The inclusion of a spin-orbit term lowers the relative spectroscopic factors for j=l+1/2 states while it increases those for j=l-1/2 states. The effect is larger for higher l values. Thus for states excited by g_{9/2} neutron pickup the relative spectroscopic factors are decreased by about 20%. Consequently, if the sum of the spectroscopic factors of the two states excited by 2p_{1/2} neutron pickup is normalized to 2 the total strength of 1g_{9/2} neutron pickup becomes 20% less than 10.0 This somewhat contradicts the expectation that N=50 is a good closed shell. On the other hand, spectroscopic factors extracted without the spin-orbit term seem to be in good agreement with the shell model in both ⁹⁰Zr and ⁸⁹Y.

C. ⁸⁶Kr(³He,α)⁸⁵Kr

For this reaction spectroscopic factors were extracted from the modified deep-well predictions only, since the same information can be expected from the predictions using the shallow well. Values obtained both with and without the spin-orbit term in the calculation of the bound-state wave function are listed in Table IV. The spectroscopic factors are normalized assuming that the 0.31-MeV state takes up the full strength for 2p_{1/2} neutron pickup. This procedure is adopted because if the spectroscopic factor of the g.s. is normalized to 10 as in the ⁸⁹Zr case, the spectroscopic factor for the 0.31-MeV state becomes larger than 2, the maximum allowed value for a 2p_{1/2} neutron pickup. The normalization factor obtained is 23 compared with 25 for ⁸⁹Y(³He,α)⁸⁸Y. The spectroscopic factor of the g.s. in ⁸⁶Kr(3/2⁺) turns out to be either 5.5 or 6.4, depending on whether the spin-orbit term is included or not. Both values seem to indicate that there are one or more l=4 states at a higher excitation energy if the g_{9/2} neutron shell is assumed to be closed. The angular distribution predicted by the DWBA for the l=3 and l=4 transitions are very similar in the present case and the determination of l values, therefore, relies on the magnitudes of the slopes of the experimental distributions; that is, l=4 transitions fall off more rapidly. Using this criterion the 1.89- and 2.03-MeV states are both likely to be l=4 states while the 2.38-MeV state is probably an l=3 state. The sum of the spectroscopic factors of all states assumed to be 3/2⁺ turns out to be 8.2 with the spin-orbit term and 10.1 without it. The theoretical value is 10.0 if the g_{9/2} neutron shell is closed. Tentative spin assignments based upon extracted spectroscopic factors and shell-model predictions are listed in Table IV.

VI. DISCUSSION

The DWBA analysis of the present (³He,α) reactions on ⁸⁹Y and ⁸⁶Kr supports the suggestion of Stock *et al.*¹⁶ concerning the selection of optical-model parameters, namely, that the optical potential for the α particles should be close to the sum of the optical potentials for

^3He and neutrons. Both the shallow and deep combinations of ^3He and α optical potential wells yield good fits to the experimental angular distributions provided that this criterion was satisfied. Spectroscopic factors extracted from both combinations agreed with each other within the extraction uncertainties of 10–20%.

The levels of ^{88}Y are very similar to those of ^{89}Zr ¹ where the $1g_{9/2}$, $2p_{1/2}$, and $2p_{3/2}$ neutron hole states make up the low-lying states (Fig. 7). In ^{88}Y these hole states couple to the $2p_{1/2}$ proton state and each splits into two levels. The total $1g_{9/2}$ neutron strength is observed in the ground and 0.25-MeV states (4^- and 5^- , respectively) in ^{88}Y . In ^{86}Kr , on the other hand, the spectroscopic factor of the g.s. ($\frac{9}{2}^+$) represents only 60% of the full $1g_{9/2}$ neutron strength. Possibly the states in ^{86}Kr at 1.89- and 2.03-MeV excitation represent some of the remaining $\frac{9}{2}^+$ hole strength. The splitting of $\frac{9}{2}^+$ neutron hole states has also been observed in ^{87}Sr by Bassani.²

In summary, spectroscopic information gathered from $(^3\text{He}, \alpha)$ reaction studies on $N=50$ nuclei has given evidence that the neutron shell is essentially closed in all the five nuclei studied. The sequence of single neu-

tron hole states, except the $1g_{9/2}$ hole state, remains the same as the proton number increases from 36 to 42. The $\frac{9}{2}^+$ neutron hole strength was found to be distributed over two or more states including the g.s. in ^{87}Sr and ^{86}Kr (where $Z \leq 38$) while for $Z > 38$ (^{88}Y , ^{89}Zr , and ^{91}Mo) the total strength seems to be in the g.s. only (or g.s. and the first excited state because of the unpaired $2p_{1/2}$ proton in ^{88}Y). According to the single-particle shell model, at $Z=38$ the $2p_{3/2}$ and $1f_{5/2}$ proton subshells are closed while both $2p_{1/2}$ and $1g_{9/2}$ subshells are open. The splitting of $\frac{9}{2}^+$ neutron hole states is probably related to the number of open proton subshells in the target. Therefore, an investigation of the proton configurations in the $N=50$ nuclei would be very interesting.

ACKNOWLEDGMENTS

The authors are indebted to R. M. Drisko for making the JULIE code available to them. They also wish to thank C. D. Goodman for sending the $^{89}\text{Y}(p, d\gamma)^{88}\text{Y}$ results prior to publication. The help by P. F. Hinrichsen in preparing this manuscript is gratefully acknowledged.

Dipole States in Sr^{88}

B. GOULARD*

Université Laval, Quebec, Canada

AND

T. A. HUGHES†‡ AND S. FALLIEROS§

Bartol Research Foundation of the Franklin Institute, Swarthmore, Pennsylvania 19081

(Received 25 July 1968)

A calculation of the dipole states in Sr^{88} is presented. In addition to the conventional one-particle-one-hole configurations, the calculation includes a set of two-particle-two-hole excitations, with the additional particle-hole pair coupled to angular momentum zero and isospin zero or one. This not only increases the number of degrees of freedom but also allows for the appearance of states with definite isospin in the final results. The dipole spectrum separates now into two groups of states with definite isospin. One group corresponds to isospin T equal to that of the ground state. It contains the giant dipole resonance of the nucleus and most of the ground-state dipole strength. The states in the second group are analog states with isospin $T+1$. They are fewer in number and lie systematically at higher energies relative to the members of the first group. They are also found to exhibit typical dipole features such as the presence of a coherent state at the high-energy side of the spectrum. The positions and the radiative strengths of the calculated levels are discussed.

I. INTRODUCTION

THE starting point for most theoretical considerations regarding the structure of nuclear dipole states is related to the observation that the electric

dipole emission or absorption of a photon by a nucleus involves the transition of a single nucleon between orbitals of different parity. Thus the absorption of a photon causes the promotion of a nucleon from an occupied to an unoccupied level, i.e., to the formation of a particle-hole pair. The various possible pairs interact with each other, and this interaction is known¹ to be

* Supported in part by the National Research Council of Canada.

† Partially supported by U. S. Office of Naval Research Contract No. 3777(00).

‡ Present address: IBM Scientific Center, Houston, Texas.

§ Supported in part by the U. S. Atomic Energy Commission.

¹ See, e.g., G. E. Brown, *Unified Theory of Nuclear Models and Forces* (North-Holland Publishing Co., Amsterdam, 1967).